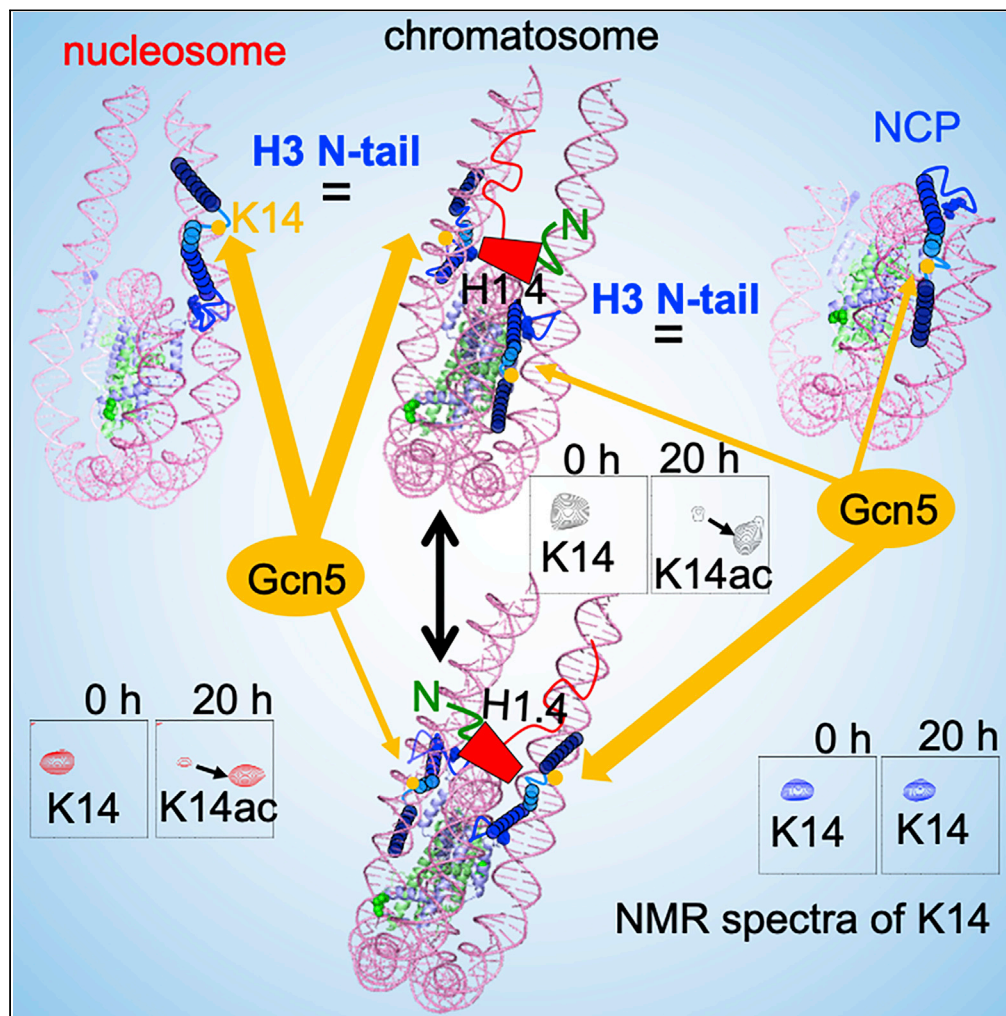


Article

Characteristic H3 N-tail dynamics in the nucleosome core particle, nucleosome, and chromosome



Ayako Furukawa,  
Masatoshi  
Wakamori,  
Yasuhiro Arimura,  
..., Hitoshi  
Kurumizaka,  
Takashi Umehara,  
Yoshifumi  
Nishimura

[nisimura@yokohama-cu.ac.jp](mailto:nisimura@yokohama-cu.ac.jp)

Highlights

H3 N-tail, restricted to two DNA gyres in NCP, binds to linker DNA in nucleosome

H4 acetylation affects the H3 N-tail dynamics in nucleosome but not in NCP

Gcn5 efficiently acetylates H3 N-tail in H4-acetylated nucleosome but not in NCP

In chromatosome, H3 N-tail adopts NCP-like and nucleosome-like conformations

Furukawa et al., iScience 25, 103937  
March 18, 2022 © 2022 The Author(s).  
<https://doi.org/10.1016/j.isci.2022.103937>



## Article

## Characteristic H3 N-tail dynamics in the nucleosome core particle, nucleosome, and chromosome

Ayako Furukawa,<sup>1</sup> Masatoshi Wakamori,<sup>2</sup> Yasuhiro Arimura,<sup>3</sup> Hideaki Ohtomo,<sup>1</sup> Yasuo Tsunaka,<sup>1</sup> Hitoshi Kurumizaka,<sup>3</sup> Takashi Umehara,<sup>2</sup> and Yoshifumi Nishimura<sup>1,4,5,\*</sup>

## SUMMARY

The nucleosome core particle (NCP) comprises a histone octamer, wrapped around by ~146-bp DNA, while the nucleosome additionally contains linker DNA. We previously showed that, in the nucleosome, H4 N-tail acetylation enhances H3 N-tail acetylation by altering their mutual dynamics. Here, we have evaluated the roles of linker DNA and/or linker histone on H3 N-tail dynamics and acetylation by using the NCP and the chromosome (i.e., linker histone H1.4-bound nucleosome). In contrast to the nucleosome, H3 N-tail acetylation and dynamics are greatly suppressed in the NCP regardless of H4 N-tail acetylation because the H3 N-tail is strongly bound between two DNA gyres. In the chromosome, the asymmetric H3 N-tail adopts two conformations: one contacts two DNA gyres, as in the NCP; and one contacts linker DNA, as in the nucleosome. However, the rate of H3 N-tail acetylation is similar in the chromosome and nucleosome. Thus, linker DNA and linker histone both regulate H3-tail dynamics and acetylation.

## INTRODUCTION

The nucleosome core particle (NCP) is a fundamental repeating unit of eukaryotic chromatin, comprising two histone H2A–H2B heterodimers and one histone (H3–H4)<sub>2</sub> tetramer, wrapped around by ~146 bp of core DNA (Luger et al., 1997). The nucleosome contains, in addition to the NCP, variable lengths of linker DNA, on which the linker histone H1 binds to produce the chromosome (Simpson, 1978; Thoma and Koller, 1977). Although X-ray crystallography and cryo-electron microscopy (cryo-EM) methods have provided detailed structures of NCPs, nucleosomes, and chromosomes, atomic-resolution structures of the histone N-tails remain elusive (Luger et al., 1997; Zhou et al., 2015; Bednar et al., 2017).

Post-translational modifications (PTMs) of histones, which mostly occur in their disordered N-terminal tails (N-tails), play essential roles in transcription, replication, recombination, and DNA repair (Fischle et al., 2003). The dynamics and PTMs of histones in NCPs, nucleosomes, and chromosomes have been examined by nuclear magnetic resonance (NMR) spectroscopy. In the nucleosome, for example, NMR has shown that the phosphorylated H3 N-tail is released from linker DNA to enhance its acetylation by the acetyltransferase Gcn5 (Liokatis et al., 2016; Stutzer et al., 2016) and, together with molecular dynamics (MD) simulations, that the H3 N-tail in the NCP interacts robustly but dynamically with core DNA (Morrison et al., 2018).

In addition, NMR recently revealed that tetra-acetylation of the H4 N-tail in the nucleosome causes dynamic structural changes in the H3 N-tail, which switches from an equilibrium of linker-DNA contact and reduced-contact states to mainly a linker-DNA contact state, resulting in its enhanced acetylation by Gcn5 (Furukawa et al., 2020). Furthermore, partial replacement of core DNA in the NCP with the phosphorylated acidic disordered (pAID) region of the histone chaperone FACT (facilitates chromatin transcription) has been shown by NMR to induce H3 N-tail exposure, which in turn accelerates K14 acetylation by Gcn5 (Tsunaka et al., 2020). The pAID-bound NCP adopts two H3 N-tail conformations: one that strongly contacts two core DNA gyres; and one that weakly contacts the site comprising pAID and core DNA, resulting in greater accessibility to Gcn5. It has also been reported that binding of linker histones to linker DNA affects the interaction between the H3 N-tail and linker DNA (Zhou et al., 2021), while our recent study based on NMR and MD simulations revealed that the N-tails of H2A and H2B in both the NCP and the nucleosome adopt two distinct conformations depending on each other (Ohtomo et al., 2021).

<sup>1</sup>Graduate School of Medical Life Science, Yokohama City University, 1-7-29 Suehiro-cho, Tsurumi-ku, Yokohama, Kanagawa 230-0045, Japan

<sup>2</sup>Laboratory for Epigenetics Drug Discovery, RIKEN Center for Biosystems Dynamics Research, 1-7-22 Suehiro-cho, Tsurumi-ku, Yokohama, Kanagawa 230-0045, Japan

<sup>3</sup>Laboratory of Chromatin Structure and Function, Institute for Quantitative Biosciences, The University of Tokyo, 1-1-1 Yayoi, Bunkyo-ku, Tokyo 113-0032, Japan

<sup>4</sup>Graduate School of Integrated Sciences for Life, Hiroshima University, 1-4-4 Kagamiyama, Higashi-Hiroshima 739-8258, Japan

<sup>5</sup>Lead contact

\*Correspondence: nisimura@yokohama-cu.ac.jp  
<https://doi.org/10.1016/j.isci.2022.103937>



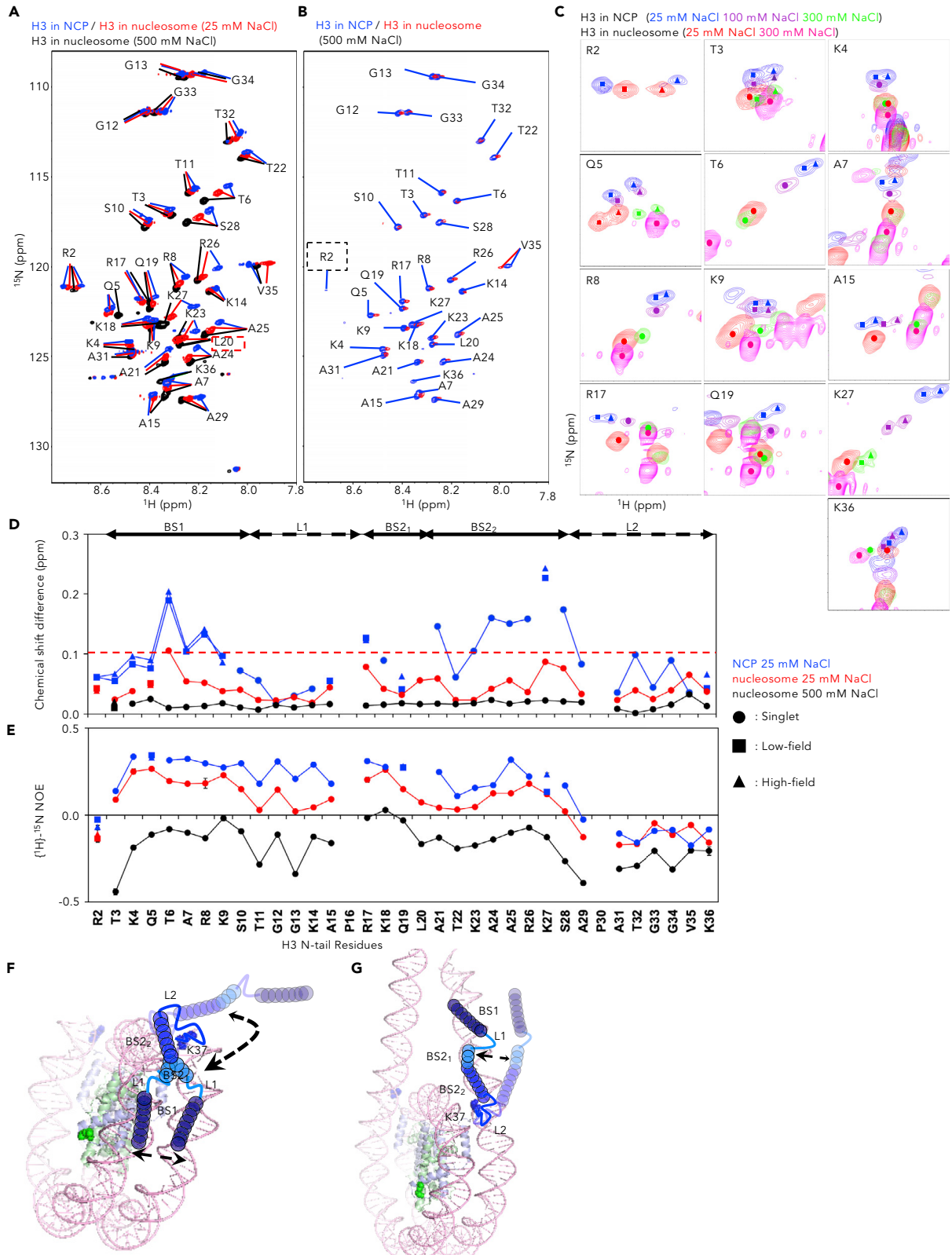


**Figure 1. Signal changes of the H3 N-tail between the NCP and nucleosome**

- (A) Superposition of  $^1\text{H}$ - $^{15}\text{N}$  HSQC spectra of the H3 N-tail in the NCP (blue) and nucleosome (red) at 25 mM NaCl and the nucleosome at 500 mM NaCl (black).
- (B) Superposition of  $^1\text{H}$ - $^{15}\text{N}$  HSQC spectra of the H3 N-tail in the NCP (blue) and nucleosome (red) at 500 mM NaCl.
- (C) Expanded spectra of 13 residues with two separate signals. Shown are signals of the NCP at 25 mM NaCl (blue), 100 mM NaCl (purple), and 300 mM NaCl (green), and the nucleosome at 25 mM NaCl (red) and 300 mM NaCl (magenta). Symbols indicate singlet signal (filled circle), high-field side of doublet signal (filled triangle), and low-field side of doublet signal (filled square).
- (D) Chemical shift differences of each residue of the H3 N-tail in the NCP at 25 mM NaCl (blue) and 500 mM NaCl (black) and in the nucleosome at 25 mM NaCl (red) with their counterparts in the nucleosome at 500 mM NaCl.
- (E) Backbone ( $^1\text{H}$ )- $^{15}\text{N}$  heteronuclear NOE values of the H3 N-tail in the NCP at 25 mM NaCl (blue), nucleosome at 25 mM NaCl (red), and nucleosome at 500 mM NaCl (black). Error bars were calculated based on the signal-to-noise ratio.
- (F) DNA interaction model of the H3 N-tail in the NCP. The H3 N-tail fluctuates dynamically between contact and non-contact states with the core DNA. The H3 N-tail from R2 to L20 (BS1, L1, and BS2<sub>1</sub>) exchanges between two forms within the two core DNA (PDB: 5av6).
- (G) DNA interaction model of the H3 N-tail in the nucleosome. The H3 N-tail binds to linker DNA non-specifically in the nucleosome (PDB: 7K61).
- See also [Figure S1](#).

So far, several studies have indicated that the H3 N-tail interacts strongly with core DNA in the NCP ([Gatchalian et al., 2017](#); [Morrison et al., 2018, 2021](#); [Tsunaka et al., 2020](#)), whereas it interacts with linker DNA in the nucleosome ([Stutzer et al., 2016](#); [Furukawa et al., 2020](#); [Zhou et al., 2021](#)). To the best of our knowledge, however, there has been no direct structural comparison of H3 N-tail dynamics in the NCP, nucleosome, and chromosome under the same or similar conditions.

In this study, we show that the dynamics of the H3 N-tail and rate of K14 acetylation by Gcn5 are greatly suppressed in the NCP, regardless of H4 N-tail acetylation, in contrast to the nucleosome, where H4 N-tail acetylation enhances both H3 N-tail dynamics and K14 acetylation. In the chromosome (i.e., linker histone H1.4-bound nucleosome), the H3 N-tail adopts two conformations—one NCP-like and one nucleosome-like—probably caused by the asymmetric binding of H1.4 to the nucleosome. However, the acetylation rate of H3 K14 in the chromosome is more similar to that in the nucleosome than that in the NCP because the two conformations are in rapid equilibrium, probably due to the binding dynamics of the linker histone H1.4.

## RESULTS

### H3 N-tail dynamics in the NCP

To explore the H3 N-tail dynamics, we first prepared 145-bp NCP and 193-bp nucleosome (with 24-bp linker DNA on both sides) containing  $^{15}\text{N}/^2\text{H}$ -labeled H3. In the NCP at 25 mM NaCl, the signals for almost all amino acids (T3–T11, K14, A15, R17–Q19, A21–A29, and T32) showed clearly a high-field shift in the  $^1\text{H}$  and/or  $^{15}\text{N}$  direction from the corresponding signals in the nucleosome at 25 mM NaCl, and a further high-field shift from the corresponding nucleosome signals at 500 mM NaCl ([Figure 1A](#)), which in turn showed a high-field shift from the corresponding signals of the H3 N-tail peptide fragment bound to DNA at 300 mM NaCl ([Figure S1A](#)). It seems likely that the H3 N-tail of the nucleosome at 500 mM NaCl is released from its DNA-contact state, because all heteronuclear NOE values of the H3 N-tail amino acids were negative, indicating that the H3 N-tail was fluctuating freely ([Figure 1E](#)). Thus, the H3 N-tail in the NCP at 25 mM NaCl strongly contacts core DNA, probably between two DNA gyres, while the H3 N-tail in the nucleosome at 25 mM NaCl weakly contacts linker DNA.

In addition, we noticed that, in the NCP, the signals for R2–K9, A15, R17, Q19, K27, and K36 were clearly split into a doublet signal and the Leu20 signal was not present. In the nucleosome, by contrast, almost all amino acids except for R2 and Q5 showed a singlet signal ([Figure 1C](#)); notably, even the H3 N-tail peptide bound to DNA showed a doublet signal only for Q5 ([Figure S1A](#)). This suggests that the H3 N-tail adopts two distinct conformations in the NCP, in contrast to its single conformation in the nucleosome. Hereafter, we clarify each doublet in the NCP as the high-field and low-field component in the  $^1\text{H}$  and/or  $^{15}\text{N}$  direction by respective h and l subscripts following the single-letter amino acid representation, for example, R2<sub>h</sub> and R2<sub>l</sub>, for R2. The salt concentration dependence of the doublet signals indicated that, in the NCP at 25 mM NaCl, both signals of the doublets correspond to DNA-contact states; in detail, however, the T6<sub>l</sub>, R8<sub>l</sub>, A15<sub>h</sub>, R17<sub>h</sub>, Q19<sub>l</sub>, and K27<sub>l</sub> components are likely to correspond to a stronger DNA-contact state, while their T6<sub>h</sub>, R8<sub>h</sub>, A15<sub>l</sub>, R17<sub>l</sub>, Q19<sub>h</sub>, and K27<sub>h</sub> counterparts seem to correspond to a slightly reduced-contact state ([Figure 1C](#)). Thus, R2–K9, A15, R17, Q19, K27, and K36 contact core DNA via two different conformations with similar affinity in the NCP at 25 mM NaCl.

Figure 1D shows the chemical shift difference (CSD) of each of the H3 N-tail amino acids in the NCP or nucleosome at 25 mM NaCl from their corresponding chemical shifts in the nucleosome at 500 mM NaCl. Based on these CSDs, the H3 N-tail of the NCP can be divided into the following sections: DNA-contact basic segment 1 (BS1, T3–S10) and basic segment 2 (BS2, R17–S28), which may be further subdivided into BS2<sub>1</sub> (R17–L20) and BS2<sub>2</sub> (A21–S28); linker L1, connecting BS1 and BS2; and linker L2, connecting BS2 to the core (Figure 1D). As compared with the nucleosome, the CSDs of the NCP were significantly larger, especially for T6, R8, R17, A21, and K23–S28, which showed a difference of more than 0.1 ppm (Figure 1D), suggesting that both BS1 and BS2, and particularly BS2<sub>2</sub>, strongly contact DNA. At 500 mM NaCl, the signals of the H3 N-tail of the NCP and nucleosome were very close to each other, except for the signal of V35 (Figures 1B and 1D), suggesting that, at high salt, the H3 N-tail in both the NCP and nucleosome is released from contact with core or linker DNA and adopts a free conformation.

Next, we conducted <sup>1</sup>H-<sup>15</sup>N heteronuclear Overhauser effect (NOE) experiments of the H3 N-tail in the NCP and nucleosome to obtain information on protein dynamics on the pico- to nano-second timescale, which reflects local conformational flexibility. The L2 region in both samples showed negative heteronuclear NOE values, but these values were significantly smaller than those of the H3 peptide bound to DNA (Figures 1E and S1B). This result suggested that L2 in the NCP and nucleosome fluctuates randomly similar to an unstructured conformation, but the fluctuations are restricted in accordance with the surrounding DNA as compared with the DNA-bound H3 peptide. BS1, L1, and BS2 in both the NCP and the nucleosome showed positive heteronuclear NOE values, indicating suppressed fluctuations. Notably, T3–S10 (BS1), T11–A15 (L1), R17, Q19 (BS2<sub>1</sub>), A21, T22, A24–R26, and S28 (BS2<sub>2</sub>) in the NCP showed higher heteronuclear NOE values relative to those in both the nucleosome and the H3 peptide bound to DNA; especially, L1 in the NCP showed significant higher values (Figures 1E and S1B). Thus, BS1, L1, and BS2 in the NCP are likely to form a more rigid rod-like structure in the NCP than in the nucleosome, owing to the binding of BS1 and BS2 to two core DNA gyres, which restricts the motion of L1. Thus, linker DNA in the nucleosome increases the flexibility of the H3 N-tail from a rigid rod-like structure in the NCP into a more flexible segmental dynamic structure consisting of BS1 and BS2 with flexible L1.

The significant CSDs and different heteronuclear NOE values of the NCP compared with the nucleosome are caused by two different DNA-contact states: namely, contact to two core DNA gyres in the NCP (Figure 1F), and contact to linker DNA in the nucleosome (Figure 1G). The H3 N-tail signals are visible owing to the dynamic fluctuation of the tail between DNA-contact and -free states. Based on the chemical shifts of the H3 N-tails in the NCP and the nucleosome, together with those of the isolated H3 peptide-free and bound to DNA, the populations of the DNA-contact states of the H3 N-tail are higher in the NCP than in the nucleosome; thus, it can be safely said that the H3 N-tail dynamically contacts DNA more strongly in the NCP than in the nucleosome.

In addition, it has been previously shown that the signals of the H3 N-tail in the NCP are nearly identical to those of the isolated H3 N-tail peptide bound to the H3 N-tail-less NCP, less similar to those of the isolated peptide bound to free DNA, and different from those of the free isolated peptide, revealing that the H3 N-tail in the NCP robustly interacts with the core DNA of the NCP (Morrison et al., 2018). In addition, our previous NMR experiments showed that, in the NCP, the asymmetric partial replacement of core DNA with the phosphorylated acidic disordered domain (pAID) of the histone chaperone FACT subunit SPT16 resulted in asymmetric environments of the two H3 N-tails: one located around two conventional core DNA gyres, which showed H3 N-tails signals corresponding to those in the conventional NCP; and the other located around the pAID and one DNA gyre. Comparing the NMR signals with those of the H3 tail peptide bound and unbound to DNA, we concluded that the H3 N-tail located in two DNA gyres contacts DNA with a much higher population of DNA-contact states as compared with the H3 N-tail located around pAID and one DNA gyre (Tsunaka et al., 2020; Figure 1F). Furthermore, we have previously shown that, in the nucleosome, the H3 N-tail probably locates around the linker DNA (Furukawa et al., 2020). Together with those experiments, our current findings indicate that the binding strength of the H3 N-tail of the NCP with core DNA is stronger than that of the nucleosome with the linker DNA (Figure S1A).

Interestingly, in the HSQC spectrum of the NCP, R2–K9, A15, R17, and Q19 showed doublet signals, and the signal of L20 (BS2<sub>1</sub>) had disappeared, but almost all signals of the amino acids after L20 were singlet except for K27 and K36 (Figure 1C). This suggests that the H3 N-tail from R2 to Q19 in the NCP adopts two different conformations within the two core DNA gyres, and the exchange rate between the two

conformations is on the intermediate or slow exchange timescale of NMR (Figure 1F). By contrast, the H3 N-tail of the nucleosome fluctuates dynamically between contact and non-contact states with the linker-DNA (Figure 1G). As previously reported, the H3 N-tail of nucleosome contacts the linker DNA using DNA-contact basic segment 1 (BS1), BS2<sub>1</sub>, and BS2<sub>2</sub> (Furukawa et al., 2020).

### K14 acetylation of the H3 N-tail in the NCP

To compare the efficiency of H3 K14 acetylation by the HAT domain of Gcn5 between the NCP and the nucleosome, we recorded time-resolved NMR spectra of K14 after the addition of Gcn5 enzyme (Figure 2A). In the nucleosome, the signal intensity of K14 gradually decreased and the signal for acetylated K14 appeared. In the NCP under the same conditions, by contrast, the signal intensity of K14 did not change during this time course (Figures 2A and 2B); thus, the rate of K14 acetylation was significantly slower in the NCP (Figure 2B). Notably, however, the CSDs due to the acetylation of K14 in the NCP and the nucleosome were similar to each other (Figures 2C and 2D), suggesting that the chemical environmental changes of the H3 N-tail induced by acetylation of K14 are similar in the two nuclear structures.

### H4 N-tail dynamics in the NCP and H4-acetylated NCP

Because there were differences in H3 N-tail dynamics between the NCP and the nucleosome, we also compared the H4 N-tail. We prepared NCPs and nucleosomes containing <sup>15</sup>N/<sup>2</sup>H-labeled H3 and <sup>15</sup>N/<sup>13</sup>C-labeled H4. Signals corresponding to R3–A15 of the H4 N-tail were observed in the HSQC spectra of both samples (Figure 3A). Almost all chemical shifts of the H4 N-tail residues were very similar between the NCP and the nucleosome at 25 mM NaCl (Figure 3B), suggesting that the H4 N-tail adopts a similar conformation in both the NCP and the nucleosome. The salt concentration-dependent chemical shift changes of the H4 N-tails between the NCP and the nucleosome were similar (Figure S2), indicating no effect of the linker DNA. This suggests that the H4 N-tails of the NCP and nucleosome fluctuate similarly between contact and non-contact states with the core DNA and the ratios of the two states depend on the salt concentration: at high salt, the non-contact state becomes the major population (Figures 3I and 3J). When the individual signal intensities were calculated as a ratio of R3 signal intensity, however, the intensity ratios of K8–K12 of the H4 N-tail were slightly higher in the NCP than in the nucleosome (Figure 3C), suggesting that the H4 N-tail is likely to adopt a slightly more flexible conformation in the NCP than in the nucleosome, although both H4 N-tails remain in a similar chemical environment.

We previously reported that the H3 N-tail in the nucleosome contacts DNA much more strongly after tetra-acetylation of the H4 N-tail (Furukawa et al., 2020). Therefore, we prepared NCP containing <sup>15</sup>N/<sup>2</sup>H-labeled H3 and <sup>15</sup>N/<sup>13</sup>C-labeled H4 with acetylated K5, K8, K12, and K16. The three signals of K5, K8, and K12 of H4 in the NCP were clearly shifted up-field in the <sup>1</sup>H direction after acetylation, and a new signal for acetylated K16 appeared, while the signals of other amino acids were slightly shifted except for R3 (Figure 3D), similar to the corresponding chemical shift changes observed in the nucleosome after H4 tetra-acetylation (Figure 3E). The appearance of a signal for acetylated K16 in the NCP and the nucleosome suggests that the tetra-acetylated H4 N-tail adopts a high flexible conformation in both as compared with the unmodified H4 N-tail, as shown in Figures 3K and 3L. In the NCP alone, however, a new R17 signal appeared after H4 acetylation (Figure 3E), suggesting that R17 in the H4 N-tail fluctuates much more in the H4-acetylated (H4ac) NCP than in the H4ac-nucleosome. Comparing the signal intensities of the H4 N-tail with and without tetra-acetylation, all residues in both the NCP and the nucleosome showed a significant increase in intensity upon H4 tetra-acetylation (Figure 3F); in other words, the H4 N-tail becomes more flexible after H4 acetylation in both the NCP and the nucleosome. This strongly suggests that the H4 N-tail in the NCP and the nucleosome is released from its DNA-contact state by H4 acetylation (Figures 3K and 3L).

In addition, after H4 tetra-acetylation, G9, L10, and G11 in the NCP showed an additional minor signal at a position similar to that observed in the nucleosome (Figure 3G). Each minor signal was close to the corresponding signal in the H4-unmodified NCP and nucleosome (Figure 3G), suggesting that the G9–G11 region adopts a minor DNA-contact state and a major reduced-contact state. The intensity ratio of the minor signal to the major signal at each residue indicated that the minor signal was a little weaker for all residues in the NCP than for their counterparts in the nucleosome (Figure 3H), suggesting that the H4 N-tail in the NCP is in contact with DNA less frequently as compared with the nucleosome. Collectively, these results show that tetra-acetylation of H4 increases the flexibility of the H4 N-tail both in the NCP and in the nucleosome, but the H4 N-tail fluctuates slightly more in the NCP than in the nucleosome.

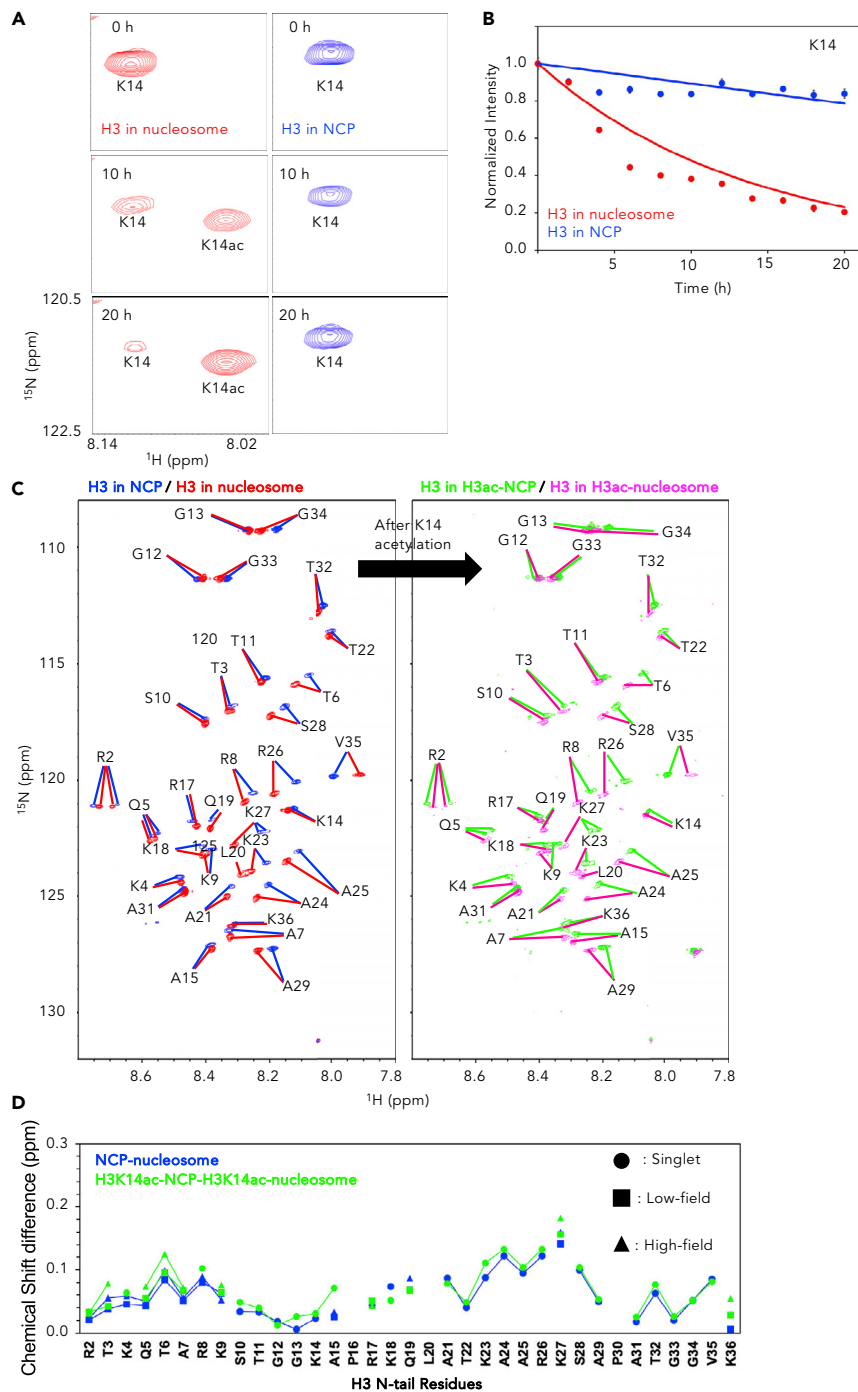


**Figure 2. Comparison of H3 K14 acetylation between the NCP and the nucleosome**

(A) Signal changes of K14 and acetylated K14 of the H3 N-tail in the NCP (blue) and nucleosome (red) after the addition of Gcn5. (B) Comparison of K14 acetylation rate in the NCP (blue circle) and nucleosome (red circle) by time-resolved NMR spectroscopy. Signal intensities were normalized by the initial signal measured before the addition of Gcn5. Blue and red lines represent the data fit to the exponential equation for the NCP and nucleosome, respectively. (C) Superposition of  $^1\text{H}$ - $^{15}\text{N}$  HSQC spectra of the H3 N-tail in the NCP (blue) and nucleosome (red), and the K14-acetylated H3 N-tail in the NCP (green) and nucleosome (pink) in 25 mM MES (6.0), 25 mM NaCl, and 2 mM DTT. (D) Chemical shift differences of H3 N-tail residues between the NCP and nucleosome (blue), and K14-acetylated H3 N-tail residues between the NCP and nucleosome (green) at 25 mM NaCl. Symbols indicate singlet signal (filled circle), high-field side of doublet signal (filled triangle), and low-field side of doublet signal (filled square).

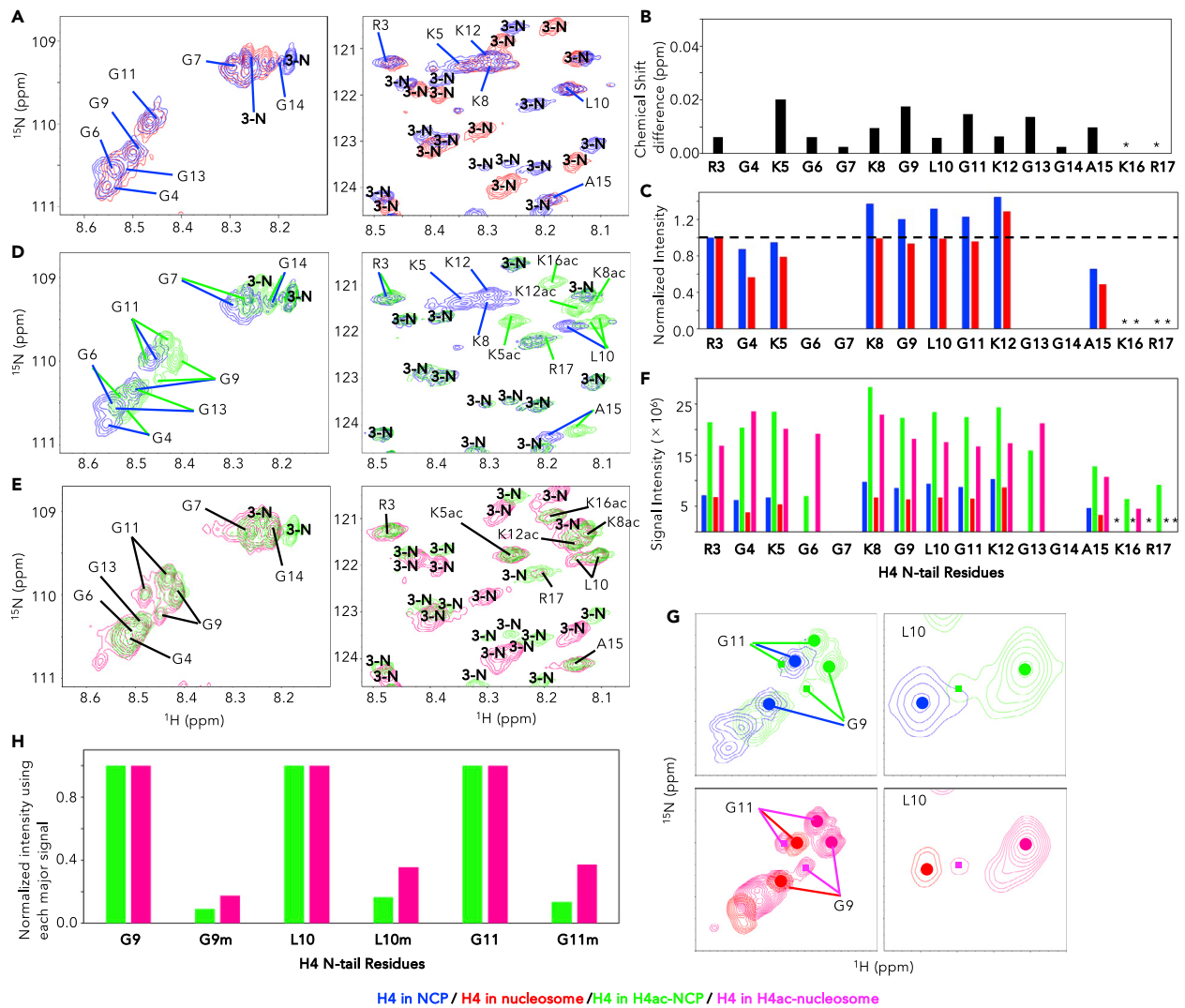


**Figure 3. Signal changes of the H4 N-tail due to H4 acetylation in the NCP and nucleosome**

- (A) Superposition of  $^1\text{H}$ - $^{15}\text{N}$  HSQC spectra of the H4 N-tail in the NCP (blue) and nucleosome (red) at 25 mM NaCl. 3-N represents signals of the H3 N-tail.
- (B) Chemical shift differences of H3 N-tail residues between the NCP and nucleosome at 25 mM NaCl. Asterisks indicate residues that were not observed.
- (C) Normalized HSQC signal intensity of each H4 N-tail residue in the NCP (blue) and nucleosome (red). Signal intensities were normalized by the respective R3 signal intensity. The intensities of G6, G7, G13, and G14 were not calculated because the signals of G6 and G7 overlapped with those of G13 and G14, respectively.
- (D) Superposition of  $^1\text{H}$ - $^{15}\text{N}$  HSQC spectra of the H4 N-tail in the NCP (blue) and H4-acetylated (H4ac) NCP (green) at 25 mM NaCl.
- (E) Superposition of  $^1\text{H}$ - $^{15}\text{N}$  HSQC spectra of the H4 N-tail in the H4ac-NCP (green) and H4ac-nucleosome (pink) at 25 mM NaCl.
- (F) Signal intensities of the H4 N-tail in the NCP (blue), H4ac-NCP (green), nucleosome (red), and H4ac-nucleosome (pink). Asterisks indicate residues that were not observed. G6 and G7 in the NCP and nucleosome overlapped with G13 and G14, respectively; G7 in the H4ac-NCP and H4ac-nucleosome overlapped with G14.
- (G) Expanded spectra of three residues of the H4 N-tail in the NCP and nucleosome. Shown are signals of the NCP (blue), H4ac-NCP (green), nucleosome (red), and H4ac-nucleosome (pink). Centers of the major and minor signals are marked with a circle and square, respectively.
- (H) Normalized signal intensities of G9, L10, and G11 residues in the H4ac-NCP (green) and H4ac-nucleosome (pink). Signal intensities were normalized by the respective major signal intensity.
- (I) DNA interaction model of the H4 N-tail in the NCP. The H4 N-tail interacts with core DNA in a highly flexible manner (PDB: 5av6).
- (J) DNA interaction model of the H4 N-tail in the nucleosome. The H4 N-tail interacts with core DNA in a highly flexible manner (PDB: 7K61).
- (K) DNA interaction model of the H4 N-tail in the H4ac-NCP. The H4-acetylated N-tail is mostly released from core DNA binding (PDB: 5av6).
- (L) DNA interaction model of the H4 N-tail in H4ac-nucleosome. The H4 N-tail in the H4ac-nucleosome is mostly released from core DNA binding (PDB: 7K61).

See also [Figure S2](#).

**H3 N-tail dynamics in the H4-acetylated NCP**

Interestingly, H4 tetra-acetylation caused no significant chemical shift changes of the H3 N-tail in the NCP in contrast to the nucleosome ([Figure 4A](#)). In addition,  $^1\text{H}$ - $^{15}\text{N}$  heteronuclear NOE values of the H3 N-tail were almost identical in NCPs with and without H4 tetra-acetylation ([Figure 4B](#)), suggesting that H4 tetra-acetylation has no effect at all on H3 N-tail dynamics in the NCP, in contrast to the H3 N-tail in the nucleosome, which is induced to adopt a rather rigid structure after H4 tetra-acetylation ([Figures 4D and 4E](#)). Regardless of whether the H4 N-tail is acetylated or not, the H3 N-tail will be dynamically fluctuating between contact and non-contact states with the core DNA ([Figure 4D](#)). On the other hand, the H3 N-tail in the H4ac-nucleosome increases its frequency of contact with DNA at a location that was previously occupied by the H4 N-tail ([Figure 4E](#)). However, the overall rigidity of the H3 N-tail in NCPs with and without H4 acetylation is much higher than that in the H4ac-nucleosome ([Figure S3](#)).

We examined whether there was a difference in the activity of H3 K14 acetylation by the HAT domain of Gcn5 between NCPs with and without H4 acetylation. As stated earlier, the acetylation rate was slowed in the NCP as compared with the nucleosome; therefore, we increased the amount of enzyme 10-fold relative to the conditions used in the nucleosome reaction. Because the signal of H3 K14 overlaps with that of H4-acetylated K8, we recorded time-resolved NMR spectra of H3 A15 in the NCP after the addition of Gcn5 ([Figure 4C](#)), and compared the rates of K14 acetylation of each H3 N-tail by using the intensity changes of A15 signals. Whereas the acetylated H4 nucleosome showed a faster acetylation rate than the unmodified nucleosome, we did not observe a significant difference in the rate of H3 N-tail K14 acetylation after H4 tetra-acetylation in the NCP ([Figures 4C and 4D](#)). This result seems reasonable because the chemical shift and heteronuclear NOE values in the NCP were not greatly altered by H4 tetra-acetylation.

**H3 N-tail dynamics in the chromosome**

There were significant chemical shift changes between the NCP and the nucleosome for the H3 N-tail, but not so much for the H4 N-tail. To examine whether the H3 N-tail adopts a similar structure in the NCP as in a heterochromatin-like structure, we added the linker histone H1.4 to the nucleosome and compared HSQC spectra of the H3 N-tail among the NCP, nucleosome, and H1.4-bound chromosome ([Figure 5A](#)). The linker histone H1.4 titration experiment confirmed that the NMR sample of the chromosome does not contain the free nucleosome ([Figure S4A](#)). After adding the linker histone, the signals of R2, S10, T11, G13, and A15 in L1, K18 and Q19 in BS2<sub>1</sub>, and all residues in BS2<sub>2</sub> shifted toward the corresponding signals of the NCP but did not overlap them ([Figures 5A, 5B, and S4A](#)). This indicated the DNA affinity of these residues is much stronger in the chromosome than in the nucleosome, but slightly weaker than that in the NCP. On the other hand, in the chromosome, the signals of S28, A29, A31, V35, and K36, located in L2 near the core, nearly overlapped with the corresponding signals of the NCP.

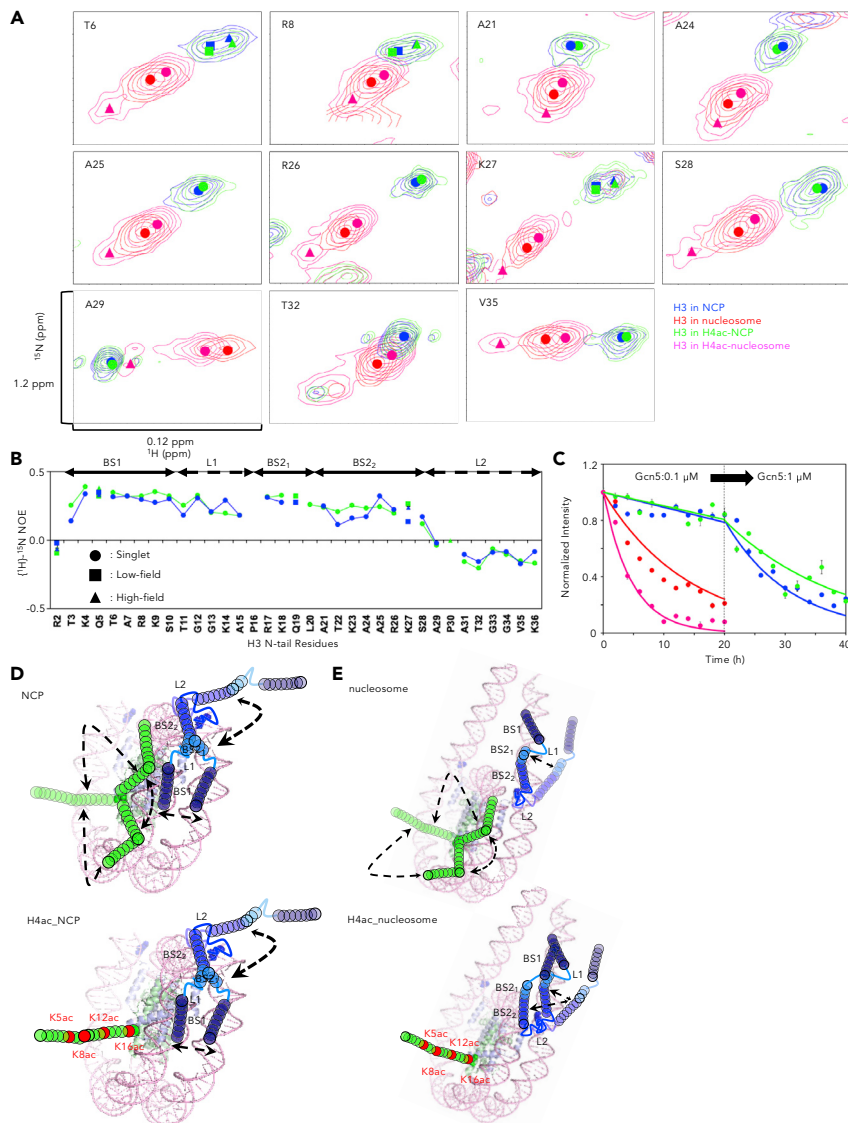


**Figure 4. Signal changes of the H3 N-tail due to H4 acetylation in the NCP and nucleosome**

(A) Expanded spectra of 11 residues of the H3 N-tail, for which minor peaks appeared after H4 acetylation in the nucleosome. Shown are signals of the NCP (blue), H4ac-NCP (green), nucleosome (red), and H4ac-nucleosome (pink). Centers of the major and minor signals are marked with a circle and triangle, respectively.

(B) Backbone  $(^1\text{H})\text{-}^{15}\text{N}$  heteronuclear NOE values of the H3 N-tail in the NCP (blue) and H4ac-NCP (green) at 25 mM NaCl. Symbols indicate singlet signal (filled circle), high-field side of doublet signal (filled triangle), and low-field side of doublet signal (filled square). Error bars were calculated based on the signal-to-noise ratio.

(C) Comparison of K14 acetylation rate by time-resolved NMR changes of A15 in the NCP (blue circle), H4ac-NCP (green circle), nucleosome (red circle), and H4ac-nucleosome (pink circle). Gcn5 enzyme was first added at 0.1  $\mu\text{M}$  and increased to 1  $\mu\text{M}$  after 20 h. Signal intensities were normalized by the initial signal recorded before the addition of Gcn5. Blue, green, red, and pink lines represent the data fit to the exponential equation for the NCP, H4ac-NCP, nucleosome, and H4ac-nucleosome, respectively.

(D) DNA interaction model of the H3 N-tail (blue) and H4-acetylated N-tail (green) in the H4ac-NCP. Regardless of whether the H4 N-tail is acetylated or not, the H3 N-tail fluctuates dynamically between contact and non-contact states with the core DNA (PDB: 5av6).

(E) DNA interaction model of the H3 N-tail (blue) and H4-acetylated N-tail (green) in the H4ac-nucleosome. The H3 N-tail in the H4ac-nucleosome makes dynamic contacts with DNA at a location that was previously occupied by the H4 N-tail (PDB: 7K61).

See also [Figure S3](#).

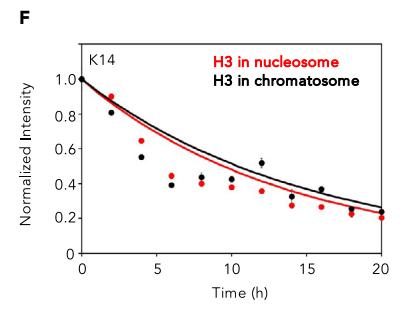
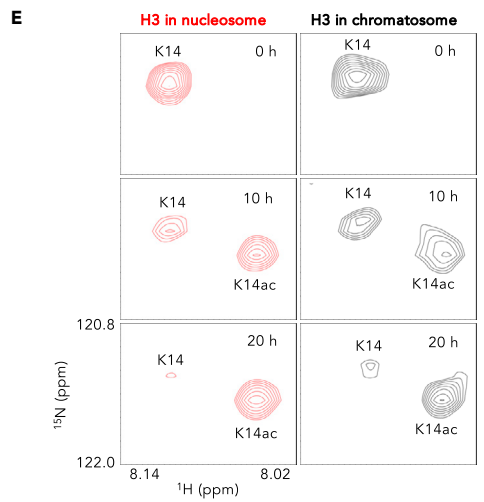
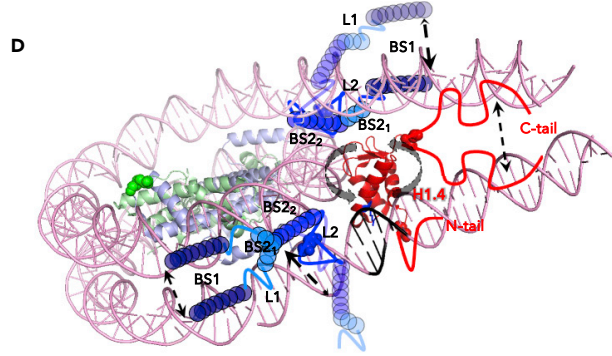
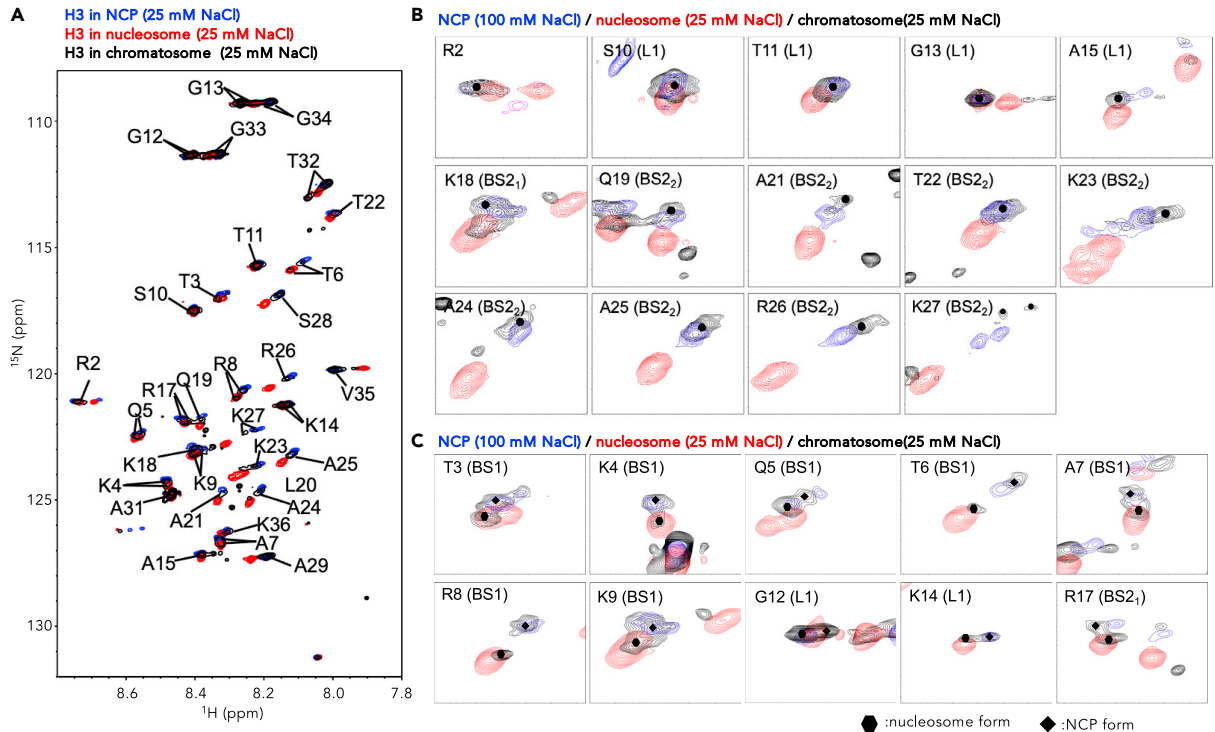


**Figure 5. Comparison of H3 N-tail signals among the chromosome, nucleosome, and NCP**

(A) Superposition of  $^1\text{H}$ - $^{15}\text{N}$  HSQC spectra of the H3 N-tail in the NCP (blue), nucleosome (red), and chromosome (i.e., nucleosome bound to H1.4; black) at 25 mM NaCl.

(B) Superposition of  $^1\text{H}$ - $^{15}\text{N}$  HSQC expanded spectra of the H3 N-tail in the NCP at 100 mM NaCl (blue), nucleosome at 25 mM NaCl (red), and chromosome (black) at 25 mM NaCl. Shown are the expanded spectra of 14 residues whose signals were shifted by the binding of H1.4.

(C) Expanded spectra of 10 residues with two signals due to binding of H1.4. Symbols indicate the NCP side of doublet signal (filled diamond) and nucleosome side of doublet signal (filled hexagon).

(D) DNA interaction model of the H3 N-tail in the chromosome. The BS<sub>2</sub> region of the H3 N-tails adopts an NCP-like form, while the BS<sub>1</sub>, L1, and BS<sub>2</sub><sub>1</sub> regions of H3 N-tails adopt two conformations: an NCP-like form and a nucleosome-like form (PDB: 7K5Y). The positions of BS<sub>2</sub> regions are likely to correspond to the H3 N-tail densities observed in the cryo-EM structure (Zhou et al., 2021).

(E) Signal changes of K14 and acetylated K14 of the H3 N-tail in the nucleosome (red) and chromosome (black) after the addition of Gcn5.

(F) Comparison of K14 acetylation rate in the nucleosome (red circle) and chromosome (black circle) by time-resolved NMR spectroscopy. Signal intensities were normalized by the initial signal measured before the addition of Gcn5. Red and black lines represent the data fit to the exponential equation for the nucleosome and chromosome, respectively.

See also Figure S4.

Interestingly, T3–K9 in BS<sub>1</sub>, G12 and K14 in L1, and R17 in BS<sub>2</sub><sub>1</sub> showed doublet signals after the addition of H1.4 (Figures 5C and S4B). In each doublet, one signal was close to the corresponding signal of the NCP and the other signal was close to the corresponding nucleosome signal, suggesting that BS<sub>1</sub>, L1, and BS<sub>2</sub><sub>1</sub> adopt two conformations—an NCP-like and nucleosome-like form—in the chromosome (Figure 5D).

As shown above, R2–K9, A15, R17, Q19, K27, and K36 showed a doublet signal in the NCP, whereas almost all amino acids except for R2 and Q5 showed a singlet signal in the nucleosome. In the chromosome, the R<sub>2h</sub>, A15<sub>L</sub>, R17<sub>L</sub>, and Q19<sub>h</sub> components of the NCP signals apparently disappeared, while the counterpart R<sub>2i</sub>, A15<sub>h</sub>, R17<sub>h</sub>, and Q19<sub>L</sub> components seemed to remain in similar chemical shift positions. Furthermore, in the chromosome, almost all of the NCP-like signals of T3–K9 in BS<sub>1</sub> showed doublet-like or broadened characters with chemical shifts similar to those of the corresponding signals of the NCP at 100 mM NaCl rather than the NCP at 25 mM NaCl (Figures 5C and S4B). This suggests that, in the NCP-like conformation of the chromosome, the H3 N-tail dynamically contacts two DNA gyres with slightly reduced affinity as compared with the NCP at 25 mM NaCl, probably because binding of H1.4 to the nucleosome is dynamic (Figure 5D).

In summary, the H1.4 titration experiment showed that segments of the H3 N-tail behave differently. While BS<sub>2</sub><sub>2</sub> shows increased DNA contact in the chromosome, the BS<sub>1</sub>, L1, and BS<sub>2</sub><sub>1</sub> regions adopt two conformations: a state of DNA contact with two DNA gyres as in the NCP, but with slightly reduced affinity; and a state of weak contact with linker DNA similar to the free nucleosome (Figure 5D).

**K14 acetylation of the H3 N-tail in the chromosome**

The above experiment showed that, in the chromosome, the H3 N-tail adopts two conformers with contact to linker DNA as in the nucleosome, and contact to two DNA gyres as in the NCP but with slightly reduced affinity. We therefore compared the activity of H3 K14 acetylation by the HAT domain of Gcn5 between the nucleosome and chromosome under the same conditions. We found, however, that the rate of K14 acetylation by Gcn5 in the chromosome was nearly identical to that in the nucleosome (Figures 5E and 5F). This strongly suggests that the two NCP-like and nucleosome-like conformations equilibrate on the timescale of the enzyme reaction, but not on the NMR or millisecond timescale.

**DISCUSSION**

In this study, we have shown that the dynamics of the H3 N-tail differ significantly between the NCP and the nucleosome. Interestingly, in the chromosome, the H3 N-tail dynamics show two forms corresponding to NCP-like and nucleosome-like conformers. Although tetra-acetylation of H4 enhances the H3 N-tail acetylation in the nucleosome, it has little effect in the NCP on the dynamics of the H3 N-tail or the rate of acetylation by Gcn5.

It is interesting to note that, in the nucleosome, the H3 N-tail favors contact to linker DNA and disfavors contact to two DNA gyres. This is probably caused by entropic effects in the linker-DNA contact state, where much more flexible binding conformations of the H3 N-tail are likely to be allowed relative to binding conformations in the two DNA gyres contact state, where the binding conformations are restricted by two DNA gyres. For the amino acids R17–Q19 (BS<sub>2</sub><sub>1</sub>) and A21–S28 (BS<sub>2</sub><sub>2</sub>), the CSD between the NCP at 25 mM

NaCl and the nucleosome at 500 mM NaCl was larger than the corresponding CSD between the nucleosome at 25 mM and the nucleosome at 500 mM NaCl (Figures 1A and 1D). This suggests that at least BS2 of the H3 N-tail in the nucleosome binds to linker DNA (Figure 1G), while BS2 in the NCP binds much more strongly to core DNA (probably two DNA gyres) than it binds to linker DNA in the nucleosome (Figure 1F). This corresponds well with earlier studies showing that the H3 N-tail in the NCP robustly binds to core DNA (Morrison et al., 2018, 2021), and that in an NCP variant in which DNA is partially by the pAID region of FACT, the H3 N-tail strongly binds to the conventional nucleosome core site formed by two DNA gyres rather than the site formed by a single DNA gyre and pAID (Tsunaka et al., 2020).

In the chromosome, the core domain of linker histone H1.4 binds around the DNA dyad site, and its C- and N-terminal tails are thought to bind to DNA (Hao et al., 2021; Zhou et al., 2015). It has been reported that R78 of H1.4 is inserted into the minor groove of linker DNA (Zhou et al., 2021); therefore, it is thought that the N-tail side of H1.4 in particular binds to linker DNA and inhibits binding of the H3 N-tail. In the chromosome, the H3 N-tail showed an asymmetric character because of H1.4 binding: on the side of the H1.4 C-tail binding to linker DNA, the H3 N-tail bound to linker DNA as in the nucleosome; and on the side of the H1.4 N-tail binding to near gyres formed by core and linker DNA, the H3 N-tail bound to two DNA gyres as in the NCP (Figure 5D). Despite this asymmetric character, the acetylation rate of H3 K14 did not differ between the chromosome and the nucleosome (Figures 5E and 5F). MD simulations have demonstrated that the globular domain of H1 in the chromosome has a highly dynamic character (Woods and Wereszczynski, 2020; Wu et al., 2021). In addition, FRAP experiments have shown that the residence time of H1 on chromatin is several minutes (Misteli et al., 2000). These results are consistent with our result that the two conformations of the H3 N-tail—namely, NCP-like and nucleosome-like conformers—equilibrate on the timescale of the acetylation enzyme reaction. The results mean that, in the presence of linker DNA and linker histone H1, the H3 N-tail is not restricted to the contact state with two core DNA gyres, but is more flexible.

Regarding the H4 N-tail, chemical shifts did not display a significant difference between the NCP and the nucleosome (Figure 3A), and the magnitude of salt concentration-dependent changes in chemical shifts of the H4 N-tail was small in both the NCP and the nucleosome (Figure S2). These results suggest the H4 N-tail is highly flexible in both the NCP and the nucleosome (Figures 3I and 3J). In addition, recent studies have reported that NMR signals of the H4 N-tail in the NCP are nearly identical to those of the free isolated peptide (Rabdano et al., 2021). According to MD simulation, the H4 N-tail can search a large surface area from superhelical location (SHL) +2 to SHL -2 on nucleosomal DNA in the NCP and the nucleosome (Rabdano et al., 2021; Peng et al., 2021). In the crystal structure of the NCP, weak electron density of the H4 N-tail is observed toward both SHL +2 (outward) and SHL -2 (inward) (Arimura et al., 2019). In the crystal structure, packing interactions between a basic H4 tail patch of K16–R19 and an acidic patch of H2A–H2B are observed between two neighboring nucleosomes (Luger et al., 1997); however, recent cryo-EM studies revealed that this H4 tail-acidic patch interaction is rarely formed in solution (Bilokapic et al., 2018). Here, although NMR signals corresponding to K16–R19 of H4 were not detected, it is certain that the R3–A15 region of the H4 N-tails is flexible.

We also compared the dynamics of H3 and H4 N-tails in the NCP and the nucleosome after tetra-acetylation of H4. The appearance of signals of K16 and/or R17 of H4 N-tail indicates that the region near the root position of the H4 N-tail is slightly released from DNA binding when the H4 N-tail is acetylated in both the NCP and the nucleosome (Figures 3K and 3L). We previously reported that the H3 N-tail in the nucleosome contacts DNA much more strongly after tetra-acetylation of the H4 N-tail (Figure 4E). Interestingly, no particular changes of the H3 N-tail in the NCP were caused by H4 tetra-acetylation (Figure 4D). SAXS and FRET experiments have shown that the ends of linker DNA approach each other when H4 N-tails are removed or acetylated. Moreover, the acetylated H4 N-tail promotes linker DNA end-to-end proximity, resulting in longer linker DNA (Andresen et al., 2013; Toth et al., 2006). Therefore, this may explain why the effect of acetylation of the H4 N-tail was observed only on the H3 N-tail in the nucleosome, and not in the NCP.

H2A N-tails bind to nucleosomal DNA at SHL  $\pm 4$ , whereas H2B N-tails are mostly bound at SHL  $\pm 3$  and SHL  $\pm 5$  (Peng et al., 2021). Thus, it is possible that H2B N-tails compete with H3 N-tails on the nucleosomal DNA gyres. On the one hand, our previous NMR study showed that the H2B N-tail adopts two different conformations that are almost identical in both the NCP and the nucleosome (Ohtomo et al., 2021): we did not detect any significant changes in the signals of the H2B N-tail between the NCP and the

nucleosome. On the other hand, the dynamic structures of the H3 N-tails in the NCP and the nucleosome differ significantly depending on the linker DNA. If there were any interactions between the H2B N-tail and the H3 N-tail, the conformations of the H2B N-tail would be also affected by the linker DNA; however, no effect of the linker DNA was observed, suggesting that the conformations of the H3 N-tail and the H2B N-tail are independent. H2A N-tails might interact with H4 N-tails on nucleosomal DNA. The H2A N-tail and H4 N-tail showed similar dynamics in both the NCP and the nucleosome independent of the linker DNA; thus, the plausible interactions between the H2A N-tail and the H4 N-tail are independent of the linker DNA, suggesting that the behavior of the H3 N-tail is independent of the interaction between the H2A and H4 N-tails.

In summary, the present study has shown that the flexibility of the H3 N-tail increases in the order of the NCP, chromosome, and the nucleosome; and both linker DNA and linker histone regulate the dynamics of the H3 N-tail. Therefore, the analysis of post-translation modifications related to heterochromatin may need to be performed using chromosome. Moreover, like the H3 N-tail, the H2A C-tail may interact dynamically with the linker DNA. In future studies, it will be interesting to use NMR to elucidate the competition for linker DNA between H2A C-tail, H3 N-tail, and linker histone H1.

### Limitations of study

Based on structural biology and *in vitro* biochemical data, we showed that the H3 N-tail dynamics is greatly affected by H4 acetylation in nucleosome but not in NCP. In addition, we showed that the H3 N-tail in chromosome adopts NCP-like and nucleosome-like conformations. To reveal the relationship between the localization of linker histone H1 and the modifications of histone H3 and H4 N-tails, additional *in vivo* data on chromosome would be required in future works.

### STAR★METHODS

Detailed methods are provided in the online version of this paper and include the following:

- KEY RESOURCES TABLE
- RESOURCE AVAILABILITY
  - Lead Contact
  - Materials availability
  - Data and code availability
- EXPERIMENTAL MODEL AND SUBJECT DETAILS
- METHOD DETAILS
  - Preparation of nucleosome
  - NMR spectrometry
  - Heteronuclear NOE experiments
  - Linker histone H1 titration experiment
  - NMR real-time monitoring of acetylation reaction
- QUANTIFICATION AND STATISTICAL ANALYSIS

### SUPPLEMENTAL INFORMATION

Supplemental information can be found online at <https://doi.org/10.1016/j.isci.2022.103937>.

### ACKNOWLEDGMENTS

This work was partly supported by Grants-in-Aid for Scientific Research on an NMR platform [07022019] (to Y.N.) from the Ministry of Education, Culture, Sports, Science and Technology (MEXT), Japan; Platform Project for Supporting Drug Discovery and Life Science Research (Basis for Supporting Innovative Drug Discovery and Life Science Research (BINDS)) from the Japan Agency for Medical Research and Development (AMED) [Grant Number JP21am0101073 (support number 0004) (to Y.N.) and grant number JP18am0101076 (to H.K.)], and JSPS KAKENHI Grant Number JP 21H05756 (to A.F.).

### AUTHOR CONTRIBUTIONS

Conceptualization, A.F. and Y.N.; Methodology, A.F. and Y.N.; Investigation, A.F., M.W., H.O., and Y.T.; Writing – Original Draft, A.F.; Writing – Review & Editing, Y.A., H.K., T.U., and Y.N.; Funding Acquisition, A.F., H.K., and Y.N.; Resources, A.F., M.W., H.O., Y.T., Y.A., T.U., H.K., and Y.N.; Supervision, Y.N.

## DECLARATION OF INTERESTS

The authors declare no competing interests.

Received: October 15, 2021

Revised: December 28, 2021

Accepted: February 14, 2022

Published: March 18, 2022

## REFERENCES

- Ahlner, A., Carlsson, M., Jonsson, B.H., and Lundstrom, P. (2013). PINT: a software for integration of peak volumes and extraction of relaxation rates. *J. Biomol. NMR* *56*, 191–202.
- Andresen, K., Jimenez-Useche, I., Howell, S.C., Yuan, C., and Qiu, X. (2013). Solution scattering and FRET studies on nucleosomes reveal DNA unwrapping effects of H3 and H4 tail removal. *PLoS One* *8*, e78587.
- Arimura, Y., Tachiwana, H., Oda, T., Sato, M., and Kurumizaka, H. (2012). Structural analysis of the hexasome, lacking one histone H2A/H2B dimer from the conventional nucleosome. *Biochemistry* *51*, 3302–3309.
- Arimura, Y., Tachiwana, H., Takagi, H., Hori, T., Kimura, H., Fukagawa, T., and Kurumizaka, H. (2019). The CENP-A centromere targeting domain facilitates H4K20 monomethylation in the nucleosome by structural polymorphism. *Nat. Commun.* *10*, 576.
- Bednar, J., Garcia-Saez, I., Boopathi, R., Cutter, A.R., Papai, G., Reymer, A., Syed, S.H., Lone, I.N., Tonchev, O., Crucifix, C., et al. (2017). Structure and dynamics of a 197 bp nucleosome in complex with linker histone H1. *Mol. Cell* *66*, 384–397.e8.
- Bilokapic, S., Strauss, M., and Halic, M. (2018). Cryo-EM of nucleosome core particle interactions in trans. *Sci. Rep.* *8*, 7046.
- Delaglio, F., Grzesiek, S., Vuister, G.W., Zhu, G., Pfeifer, J., and Bax, A. (1995). NMRPipe: a multidimensional spectral processing system based on UNIX pipes. *J. Biomol. NMR* *6*, 277–293.
- Fischle, W., Wang, Y., and Allis, C.D. (2003). Histone and chromatin cross-talk. *Curr. Opin. Cell Biol.* *15*, 172–183.
- Furukawa, A., Wakamori, M., Arimura, Y., Ohtomo, H., Tsunaka, Y., Kurumizaka, H., Umehara, T., and Nishimura, Y. (2020). Acetylated histone H4 tail enhances histone H3 tail acetylation by altering their mutual dynamics in the nucleosome. *Proc. Natl. Acad. Sci. U S A* *117*, 19661–19663.
- Gatchalian, J., Wang, X., Ikebe, J., Cox, K.L., Tencer, A.H., Zhang, Y., Burge, N.L., Di, L., Gibson, M.D., Musselman, C.A., et al. (2017). Accessibility of the histone H3 tail in the nucleosome for binding of paired readers. *Nat. Commun.* *8*, 1489.
- Hao, F., Kale, S., Dimitrov, S., and Hayes, J.J. (2021). Unraveling linker histone interactions in nucleosomes. *Curr. Opin. Struct. Biol.* *71*, 87–93.
- Ishiyama, S., Nishiyama, A., Saeki, Y., Moritsugu, K., Morimoto, D., Yamaguchi, L., Arai, N., Matsumura, R., Kawakami, T., Mishima, Y., et al. (2017). Structure of the Dnmt1 reader module complexed with a unique two-mono-ubiquitin mark on histone H3 reveals the basis for DNA methylation maintenance. *Mol. Cell* *68*, 350–360.e7.
- Johnson, B.A., and Blevins, R.A. (1994). NMR view: a computer program for the visualization and analysis of NMR data. *J. Biomol. NMR* *4*, 603–614.
- Kay, L.E., Torchia, D.A., and Bax, A. (1989). Backbone dynamics of proteins as studied by 15N inverse detected heteronuclear NMR spectroscopy: application to staphylococcal nuclease. *Biochemistry* *28*, 8972–8979.
- Kobayashi, N., Iwahara, J., Koshiba, S., Tomizawa, T., Tochio, N., Guntert, P., Kigawa, T., and Yokoyama, S. (2007). KJIRA, a package of integrated modules for systematic and interactive analysis of NMR data directed to high-throughput NMR structure studies. *J. Biomol. NMR* *39*, 31–52.
- Liokatis, S., Klingberg, R., Tan, S., and Schwarzer, D. (2016). Differentially isotope-labeled nucleosomes to study asymmetric histone modification crosstalk by time-resolved NMR spectroscopy. *Angew. Chem. Int. Ed. Engl.* *55*, 8262–8265.
- Lowary, P.T., and Widom, J. (1998). New DNA sequence rules for high affinity binding to histone octamer and sequence-directed nucleosome positioning. *J. Mol. Biol.* *276*, 19–42.
- Luger, K., Mader, A.W., Richmond, R.K., Sargent, D.F., and Richmond, T.J. (1997). Crystal structure of the nucleosome core particle at 2.8 Å resolution. *Nature* *389*, 251–260.
- Machida, S., Hayashida, R., Takaku, M., Fukuto, A., Sun, J., Kinomura, A., Tashiro, S., and Kurumizaka, H. (2016). Relaxed chromatin formation and weak suppression of homologous pairing by the testis-specific linker histone H1T. *Biochemistry* *55*, 637–646.
- Misteli, T., Gunjan, A., Hock, R., Bustin, M., and Brown, D.T. (2000). Dynamic binding of histone H1 to chromatin in living cells. *Nature* *408*, 877–881.
- Moriwaki, Y., Yamane, T., Ohtomo, H., Ikeguchi, M., Kurita, J., Sato, M., Nagadoi, A., Shimojo, H., and Nishimura, Y. (2016). Solution structure of the isolated histone H2A-H2B heterodimer. *Sci. Rep.* *6*, 24999.
- Morrison, E.A., Baweja, L., Poirier, M.G., Wereszczynski, J., and Musselman, C.A. (2021). Nucleosome composition regulates the histone H3 tail conformational ensemble and accessibility. *Nucleic Acids Res.* *49*, 4750–4767.
- Morrison, E.A., Bowerman, S., Sylvers, K.L., Wereszczynski, J., and Musselman, C.A. (2018). The conformation of the histone H3 tail inhibits association of the BPTF PHD finger with the nucleosome. *Elife* *7*, e31481.
- Ohtomo, H., Kurita, J.I., Sakuraba, S., Li, Z., Arimura, Y., Wakamori, M., Tsunaka, Y., Umehara, T., Kurumizaka, H., Kono, H., et al. (2021). The N-terminal tails of histones H2A and H2B adopt two distinct conformations in the nucleosome with contact and reduced contact to DNA. *J. Mol. Biol.* *433*, 167110.
- Peng, Y., Li, S., Onufriev, A., Landsman, D., and Panchenko, A.R. (2021). Binding of regulatory proteins to nucleosomes is modulated by dynamic histone tails. *Nat. Commun.* *12*, 5280.
- Rabdano, S.O., Shannon, M.D., Izmailov, S.A., Gonzalez Salguero, N., Zandian, M., Purusottam, R.N., Poirier, M.G., Skrynnikov, N.R., and Jaroniec, C.P. (2021). Histone H4 tails in nucleosomes: a fuzzy interaction with DNA. *Angew. Chem. Int. Ed. Engl.* *60*, 6480–6487.
- Simpson, R.T. (1978). Structure of the chromatosome, a chromatin particle containing 160 base pairs of DNA and all the histones. *Biochemistry* *17*, 5524–5531.
- Stutzer, A., Liokatis, S., Kiesel, A., Schwarzer, D., Sprangers, R., Soding, J., Selenko, P., and Fischle, W. (2016). Modulations of DNA contacts by linker histones and post-translational modifications determine the mobility and modifiability of nucleosomal H3 tails. *Mol. Cell* *61*, 247–259.
- Sugase, K., Konuma, T., Lansing, J.C., and Wright, P.E. (2013). Fast and accurate fitting of relaxation dispersion data using the flexible software package GLOVE. *J. Biomol. NMR* *56*, 275–283.
- Thoma, F., and Koller, T. (1977). Influence of histone H1 on chromatin structure. *Cell* *12*, 101–107.
- Toth, K., Brun, N., and Langowski, J. (2006). Chromatin compaction at the mononucleosome level. *Biochemistry* *45*, 1591–1598.
- Tsunaka, Y., Ohtomo, H., Morikawa, K., and Nishimura, Y. (2020). Partial replacement of nucleosomal DNA with human FACT induces dynamic exposure and acetylation of histone H3 N-terminal tails. *iScience* *23*, 101641.
- Wakamori, M., Fujii, Y., Suka, N., Shirouzu, M., Sakamoto, K., Umehara, T., and Yokoyama, S. (2015). Intra- and inter-nucleosomal interactions of the histone H4 tail revealed with a human nucleosome core particle with genetically-incorporated H4 tetra-acetylation. *Sci. Rep.* *5*, 17204.

Woods, D.C., and Wereszczynski, J. (2020). Elucidating the influence of linker histone variants on chromosome dynamics and energetics. *Nucleic Acids Res.* 48, 3591–3604.

Wu, H., Dalal, Y., and Papoian, G.A. (2021). Binding dynamics of disordered linker histone H1

with a nucleosomal particle. *J. Mol. Biol.* 433, 166881.

Zhou, B.R., Feng, H., Kale, S., Fox, T., Khant, H., de Val, N., Ghirlando, R., Panchenko, A.R., and Bai, Y. (2021). Distinct structures and dynamics of chromatosomes with different

human linker histone isoforms. *Mol. Cell* 81, 166–182.e6.

Zhou, B.R., Jiang, J., Feng, H., Ghirlando, R., Xiao, T.S., and Bai, Y. (2015). Structural mechanisms of nucleosome recognition by linker histones. *Mol. Cell* 59, 628–638.

## STAR★METHODS

### KEY RESOURCES TABLE

REAGENT or RESOURCE	SOURCE	IDENTIFIER
<b>Bacterial and virus strains</b>		
One Shot™™ BL21(DE3) cells	Thermo Fisher	Cat#C600003
One Shot™™ TOP10 cells	Thermo Fisher	Cat#C404010
BL21-CodonPlus (DE3)-RIL competent cells	Agilent Technologies	Cat#230245
<b>Chemicals, peptides, and recombinant proteins</b>		
Recombinant human H3 histone	<a href="#">Tsunaka et al., 2020</a>	N/A
Recombinant human H1.4 histone	<a href="#">Machida et al., 2016</a>	N/A
Recombinant human H4 histones	<a href="#">Wakamori et al., 2015</a>	N/A
Recombinant human H2A/H2B histones	<a href="#">Moriwaki et al., 2016</a>	N/A
Recombinant human H3 peptide	<a href="#">Ishiyama et al., 2017</a>	N/A
Recombinant human Gcn5 catalytic domain	Enzo Life Sciences	Cat#BML-SE272-0050
SYBR Gold Nucleic Acid Gel Stain	Thermo Fisher	Cat#S11494
<b>Deposited data</b>		
Human nucleosome core particle	<a href="#">Wakamori et al., 2015</a>	5AV6
Cryo-EM structure of 197 bp nucleosome aided by scFv	<a href="#">Zhou et al., 2021</a>	7K61
Cryo-EM structure of a chromatosome containing human linker histone H1.4	<a href="#">Zhou et al., 2021</a>	7K5Y
<b>Oligonucleotides</b>		
33-mer 601_1 5'-ATCAGAATCCCGGTGCCGAGGCC GCTCAATTGG-3'	Thermo Fisher	N/A
33-mer 601_2 5'-CCAATTGAGCGCCTCGGCACCG GGATTCTGAT-3'	Thermo Fisher	N/A
<b>Recombinant DNA</b>		
pET-H2A	<a href="#">Moriwaki et al., 2016</a>	N/A
pET-H2B	<a href="#">Moriwaki et al., 2016</a>	N/A
pET-H3.1	<a href="#">Tsunaka et al., 2020</a>	N/A
pCR2.1-H4, pET-H4	<a href="#">Wakamori et al., 2015</a>	N/A
pET-H1.4	<a href="#">Machida et al., 2016</a>	N/A
pGEX-ST1-histone H3 (residues 1-36+37W)	<a href="#">Ishiyama et al., 2017</a>	N/A
Tvector-145-bp 601 DNA	<a href="#">Tsunaka et al., 2020</a>	N/A
pGEM-T easy -193-bp 601	<a href="#">Arimura et al., 2012</a>	N/A
<b>Software and algorithms</b>		
NMRPipe	<a href="#">Delaglio et al., 1995</a>	<a href="https://www.ibbr.umd.edu/nmrpipe/install.html">https://www.ibbr.umd.edu/nmrpipe/install.html</a>
Magro	<a href="#">Kobayashi et al., 2007</a>	
Glove	<a href="#">Sugase et al., 2013</a>	Ver3
NMR View J	One Moon Scientific, Inc	
PINT	<a href="#">Ahlner et al., 2013</a>	
Pymol	Schrodinger	Ver 2.5.1

## RESOURCE AVAILABILITY

### Lead Contact

Further information and requests for resources and reagents should be directed to and will be fulfilled by the Lead Contact, Dr. Yoshifumi Nishimura ([nisimura@yokohama-cu.ac.jp](mailto:nisimura@yokohama-cu.ac.jp)).

### Materials availability

This study did not generate new unique reagents.

### Data and code availability

This study did not generate datasets and code.

## EXPERIMENTAL MODEL AND SUBJECT DETAILS

All genes were subcloned into expression plasmids and expressed in *Escherichia coli*.

## METHOD DETAILS

### Preparation of nucleosome

The two DNA fragments of 145 and 193 bp were based on the Widom 601 sequence (Lowary and Widom, 1998) and purified as previously described (Arimura et al., 2012). Unlabeled human H2A and H2B histones were expressed and purified as previously described (Moriwaki et al., 2016).  $^2\text{H}/^{15}\text{N}/^{13}\text{C}$ - and  $^2\text{H}/^{15}\text{N}$ -labeled human H3 histone was expressed and purified by a published method (Tsunaka et al., 2020).  $^{13}\text{C}/^{15}\text{N}$ -labeled or unlabeled H4 and H4 containing acetyl-lysine (Taiyo Nissan Co. Ltd.) were synthesized by cell-free protein synthesis (Wakamori et al., 2015). The H4-acetylated and unmodified nucleosomes were reconstituted as described (Wakamori et al., 2015). His6-SUMO-tagged H1.4 protein was produced in *E. coli* BL21 (DE3) cells, carrying the minor tRNA expression vector (Codon(+))RIL as described previously (Machida et al., 2016).

The reconstructed NCP, H4ac\_NCP, nucleosome, and H4ac\_nucleosome were analyzed by native PAGE, using a gel containing 6% acrylamide (acrylamide: bisacrylamide = 59:1) in 0.2 × TBE buffer, and subsequent staining with ethidium bromide (Life Technologies) (Figure S5A).

### NMR spectrometry

NMR experiments were performed on AVANCE 600-MHz and AVANCE III HD 950-MHz spectrometers with a triple-resonance TCI cryogenic probe (Bruker Bio Spin) at 298 K using 20–110 μM samples dissolved in 25 mM MES (pH 6.0), 25–500 mM NaCl, 2 mM DTT, and 5% D<sub>2</sub>O. Three-dimensional transverse relaxation optimized spectroscopy (TROSY) of HNCO, HN(CA)CO, HNCA, HN(CO)CA, HNCACB, and HN(CO)CACB was used to obtain sequential assignments of the backbone  $^1\text{H}$ ,  $^{13}\text{C}$ , and  $^{15}\text{N}$  chemical shifts of the H3 and H4 N-tails in the NCP and nucleosome. NMR data were processed by NMRPipe (Delaglio et al., 1995), and analyzed by Magro (Kobayashi et al., 2007), NMRViewJ (Johnson and Blevins, 1994: One Moon Scientific, Inc., Westfield, NJ, USA), and PINT (Ahlner et al., 2013). Averaged chemical shift differences were calculated by the equation  $[(\Delta\text{HN})^2 + (\Delta\text{N}/5)^2]^{1/2}$ , where  $\Delta\text{HN}$  and  $\Delta\text{N}$  are chemical shift differences of the amide proton and nitrogen atoms, respectively.

### Heteronuclear NOE experiments

$\{^1\text{H}\}$ - $^{15}\text{N}$  heteronuclear NOE experiments of  $^2\text{H}/^{15}\text{N}$ -labeled H3 in the nucleosome were performed at 298 K on an AVANCE 600-MHz spectrometer (Kay et al., 1989).  $\{^1\text{H}\}$ - $^{15}\text{N}$  heteronuclear NOE values were calculated from the intensity ratio of signals in spectra acquired with and without pre-saturation of the amide protons. Errors in NOE measurements were estimated on the basis of root-mean-squared values of the background noise.

### Linker histone H1 titration experiment

The unlabeled linker histone H1.4 was added step-by-step so as to reach the ratios of 0.15, 0.3, 0.5, 1.0, and 1.5 to the nucleosome containing  $^{15}\text{N}/^2\text{H}$ -labeled H3. In each step, the precipitation that occurred during the titration process was removed and the  $^1\text{H}$ - $^{15}\text{N}$  HSQC spectrum of the supernatant of the nucleosome/H1.4 solution was acquired at 298K. In the  $^1\text{H}$ - $^{15}\text{N}$  HSQC spectrum with 1.5 equiv of H1.4 added, we confirmed that there were no signals of nucleosome, indicating all the nucleosomes in the NMR solution were the

H1-bound form (chromatosome) (Figure S4A). Nucleosomes with linker histone H1.4 added in ratios of 0.5, 1.0, and 1.5 were confirmed by electrophoresis at 4°C on a 7.5% native-PAGE in 1 Tris-glycine buffer with visualization by SYBR Gold nucleic acid gel stain (Figure S6).

### NMR real-time monitoring of acetylation reaction

Acetylation of H3 K14 in the nucleosome, H4ac-nucleosome, and chromatosome (20 μM) were carried out in 25 mM NaPB (pH 6.8), 25 mM NaCl, 2 mM DTT, and 5% D<sub>2</sub>O with 250 μM acetyl-CoA and 100 nM Gcn5 (Enzo Life Sciences) at 303 K. Acetylation of H3 K14 in the NCP and H4ac-NCP (20 μM) were carried out with 250 μM acetyl-CoA and 1 μM Gcn5 (Enzo Life Sciences) at 303 K. Modification reactions were monitored by <sup>1</sup>H-<sup>15</sup>N TROSY-HSQC NMR experiments. The signal intensities obtained were fitted to the exponential equation by using the program GLOVE (Sugase et al., 2013).

### QUANTIFICATION AND STATISTICAL ANALYSIS

The intensities and chemical shifts of signals in NMR spectra were quantified using Magro (Kobayashi et al., 2007), NMRViewJ (One Moon Scientific, Inc., Westfield, NJ, USA), and PINT (Ahlner et al., 2013). Averaged chemical shift differences were calculated by the equation  $[(\Delta\text{HN})^2 + (\Delta\text{N}/5)^2]^{1/2}$ . Errors in NOE measurements were estimated on the basis of root-mean-squared values of the background noise. The signal intensities obtained by NMR real-time monitoring were fitted to the exponential equation by using the program GLOVE (Sugase et al., 2013).